



## *Ab initio* electronic structure of solid coronene: Differences from and commonalities to picene

Taichi Kosugi,<sup>1</sup> Takashi Miyake,<sup>1,2</sup> Shoji Ishibashi,<sup>1</sup> Ryotaro Arita,<sup>2,3,4</sup> and Hideo Aoki<sup>5</sup>

<sup>1</sup>Nanosystem Research Institute "RICS", AIST, Umezono, Tsukuba 305-8568, Japan

<sup>2</sup>Japan Science and Technology Agency, CREST, Honcho, Kawaguchi, Saitama 332-0012, Japan

<sup>3</sup>Department of Applied Physics, University of Tokyo, Hongo, Tokyo 113-8656, Japan

<sup>4</sup>PRESTO, Japan Science and Technology Agency (JST), Kawaguchi, Saitama 332-0012, Japan

<sup>5</sup>Department of Physics, University of Tokyo, Hongo, Tokyo 113-0033, Japan

(Received 2 May 2011; revised manuscript received 29 May 2011; published 20 July 2011)

We have obtained the first-principles electronic structure of solid coronene, which has been recently reported to exhibit superconductivity with potassium doping. Since coronene, along with picene, the first aromatic superconductor, now provides a class of superconductors as solids of aromatic compounds, here we compare the two cases by examining the electronic structures. In the undoped coronene crystal, where the molecules are arranged in a herringbone structure with two molecules in a unit cell, the conduction band above an insulating gap is found to comprise four bands, which basically originate from the lowest two unoccupied molecular orbitals (doubly-degenerate, reflecting the high symmetry of the molecular shape) in an isolated molecule but the bands are entangled as in solid picene. The Fermi surface for a candidate of the structure of  $K_x$  coronene with  $x = 3$ , for which superconductivity is found, comprises multiple sheets, as in doped picene but exhibiting a larger anisotropy with different topology.

DOI: [10.1103/PhysRevB.84.020507](https://doi.org/10.1103/PhysRevB.84.020507)

PACS number(s): 74.20.Pq, 74.70.Kn, 74.70.Wz

**Introduction.** The discovery of superconductivity in solid picene doped with potassium atoms<sup>1</sup> is seminal and came as a surprise since picene, having the highest  $T_c$  among organic superconductors, belongs to the class of *aromatic* compounds, the most typical, textbook class of organic materials. A natural question to ask is whether other aromatic compounds can become superconducting as well. Before examining this question, let us first briefly summarize the known superconductors in carbon-based materials. The first discovery goes back to 1965, when a graphite-intercalation compound (GIC),  $KC_8$ , was found to be a superconductor at 0.1 K;<sup>2</sup> the highest  $T_c$  among GICs to date is 11.6 K in  $CaC_6$ .<sup>3</sup> Fullerene is another class, where potassium-doped fullerene,  $K_3C_{60}$ , has  $T_c = 20$  K,<sup>4</sup> followed by  $Cs_2RbC_{60}$  with  $T_c = 33$  K,<sup>5</sup> or 40 K in  $Cs_3C_{60}$  under 15 kbar.<sup>6</sup> In the last decade, boron-doped diamond<sup>7</sup> joined carbon-based superconductors. The first aromatic superconductivity in potassium-doped solid picene discovered by Kubozono's group,<sup>1</sup> with  $T_c = 7$ –18 K in  $K_x$  picene for  $x \simeq 3$ , was unsuspected, since the (undoped) solid of picene (a hydrocarbon compound with five benzene rings connected in a zigzag) has been known to be a good insulator, as naturally expected for an aromatic molecule.

The present authors have reported the first-principles electronic structure of both undoped and doped solid picene in the framework of density functional theory (DFT) within the local density approximation (LDA).<sup>8</sup> We have revealed, for undoped solid picene, where picene molecules take a herringbone structure, that the conduction band consists of four bands, which originate basically from the lowest two unoccupied molecular orbitals (LUMO and LUMO+1) of an isolated molecule, but the bands are entangled (i.e., they cross each other). When doped with potassium atoms, the herringbone structure is deformed, and the electronic wave function significantly spills from the organic molecules' LUMOs into potassium sites.<sup>8</sup>

Now, if we return to the question of whether and which other aromatic compounds can become superconducting,

recently Kubozono's group reported superconductivity in doped coronene.<sup>9</sup> Coronene,  $C_{24}H_{12}$ , is another typical aromatic molecule, with seven benzene rings assembled in a concentric disk. Superconductivity in  $K_x$  coronene is reported to appear around  $x \simeq 3$  with  $T_c$  up to 15 K.<sup>10</sup> Motivated by this, here we have obtained the electronic structure of solid coronene, both undoped and doped. Of obvious interest are the differences and commonalities between the crystal and electronic structures of solid coronene as compared with those of solid picene. This is precisely the purpose of the present work. The obtained results are analyzed with maximally-localized Wannier functions (WFs),<sup>11</sup> in terms of which we downfold the system into a tight-binding model and compare with those for picene.

We shall show that the conduction band of undoped solid coronene comprises four bands, which basically originate from the two LUMOs (doubly-degenerate, reflecting the symmetry of a molecule higher than that of picene) in an isolated molecule, but the bands are entangled as in solid picene. The Fermi surface for a candidate of the structure of  $K_x$  coronene with  $x = 3$ , for which superconductivity is found, comprises multiple sheets, as in doped picene but exhibiting a more one-dimensional character with different anisotropy and topology.

The present electronic structure will serve as a basis for discussing mechanisms of superconductivity. Since some classes of organic superconductors are considered to have an electronic mechanism,<sup>12</sup> picene and coronene superconductors may possibly belong to them. There have been some theoretical studies<sup>13,14</sup> that suggest that solid picene is a strongly correlated electron system. For the electron-phonon coupling, on the other hand, Kato *et al.* estimated the phonon frequencies and the electron-phonon coupling for various hydrocarbon molecules.<sup>15</sup> For picene they found that the electron-phonon coupling can be as large as 0.2 eV. While it is generally difficult to quantitatively estimate  $T_c$  for a phonon mechanism due to the ambiguity in the Coulomb pseudopotential ( $\mu^*$ ), they concluded that  $T_c \sim 10$  K may be expected. They also

estimated the coupling for coronene to be about 0.1 eV. Subedi and Boeri<sup>16</sup> recently calculated the phonon spectrum and electron-phonon interaction for solid picene, and they found that the calculated electron-phonon coupling,  $-0.2$  eV, is sufficiently strong to reproduce the experimental  $T_c$  of 18 K within the Migdal-Eliashberg theory.

**First-principles bands.** The calculation is based on DFT, where LDA in the Perdew-Zunger formula is adopted for the exchange-correlation energy functional.<sup>17</sup> We use the projector-augmented wave (PAW) method,<sup>18</sup> implemented to the Quantum Materials Simulator (QMAS) package.<sup>19</sup> The pseudo Bloch wave functions are expanded by plane waves up to an energy cutoff of 40 Ry with  $4 \times 6 \times 4$   $k$  points.

For the crystal structure, here we adopt the experimental lattice parameters of natural coronene (karpatite) reported by Echigo *et al.*<sup>20</sup> Natural coronene has a monoclinic (space group of  $P2_1/a$ ) structure with  $a = 16.094$ ,  $b = 4.690$ , and  $c = 10.049$  Å, and  $\beta = 110.79^\circ$ . We have also performed calculations adopting the lattice parameters of synthetic coronene<sup>21</sup> and have confirmed that the results are essentially unchanged from those for natural coronene. The molecular solid has a herringbone arrangement of molecules as depicted in Fig. 1 with a unit cell containing two molecules [centered respectively at  $(0,0,0)$  and  $(1/2,1/2,0)$  as dictated by the symmetry]. The lattice parameters are fixed at the experimental values, and the internal atomic positions are optimized.<sup>22</sup> The angle between the planes of the inequivalent molecules in the optimized geometry is  $95^\circ$ , which agrees with the measured value. It was found that the point-group symmetry  $D_{6h}$  for an isolated coronene molecule is lowered to  $D_{2h}$  in the crystal.

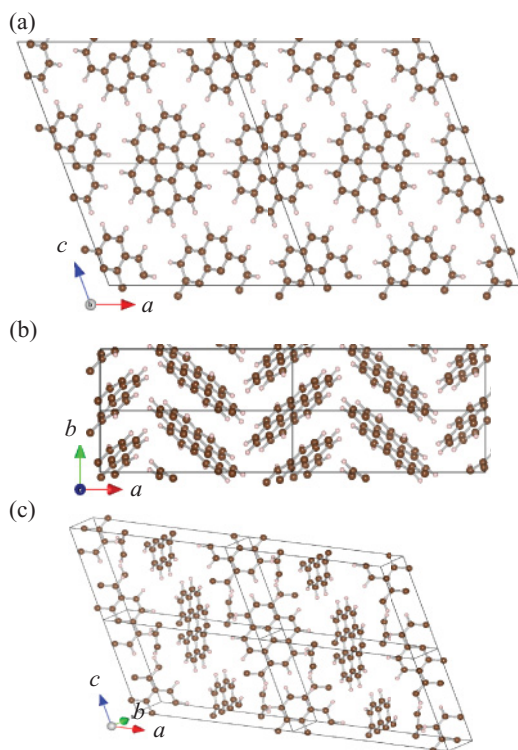


FIG. 1. (Color online) Crystal structure of undoped solid coronene viewed along (a) the  $b$  axis and (b) the  $c$  axis, and (c) a bird's eye view. Solid lines delineate unit cells.

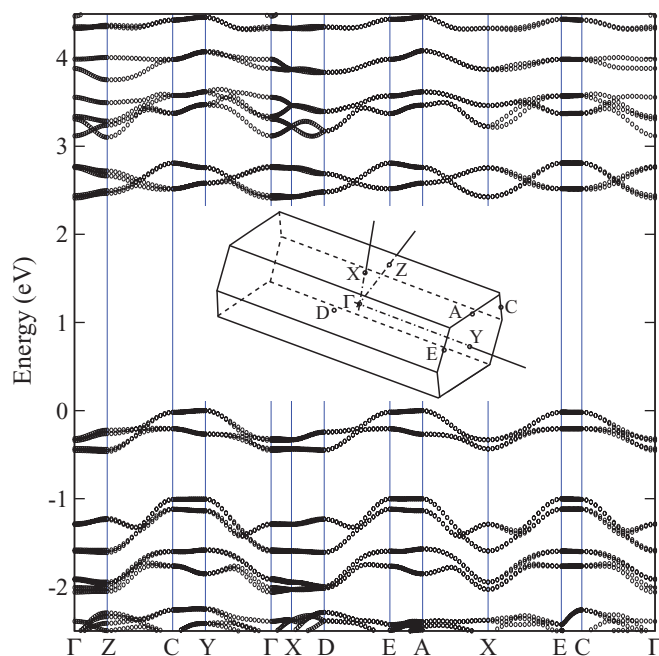


FIG. 2. (Color online) Calculated electronic band structure of the undoped crystalline coronene. The origin of the energy is set to be the valence band top. The inset depicts the Brillouin zone with  $\Gamma$ , Z, C, Y, X, D, E, and A, respectively, corresponding to  $(0,0,0)$ ,  $(0,0,1/2)$ ,  $(0,1/2,1/2)$ ,  $(0,1/2,0)$ ,  $(1/2,0,0)$ ,  $(1/2,0,1/2)$ ,  $(1/2,1/2,1/2)$ , and  $(1/2,1/2,0)$  in units of  $(\mathbf{a}^*, \mathbf{b}^*, \mathbf{c}^*)$ .

Figure 2 displays the electronic band structure of coronene. We have an insulator with a band gap of 2.41 eV. The gap, which is naturally smaller than the HOMO-LUMO gap, calculated to be 2.90 eV, of an isolated coronene molecule, is indirect, with the valence band top located at Y in the Brillouin zone, while the conduction band bottom is at  $\Gamma$ . Since the crystal structure is layered, with a herringbone arrangement, on the  $a$ - $b$  plane, of molecules stacked along  $c$  axis, the electronic structure is more dispersive along the  $a^*$ - $b^*$  axis. More precisely, the dispersion along  $b^*$  is larger than that for  $a^*$ , which directly reflects the distance between neighboring molecules being shortest along  $b$ . The conduction band, with a width of 0.40 eV, consists of four bands derived from the doubly-degenerate  $e_{1g}$  LUMOs. For solid picene by comparison, the conduction band, with a width 0.39 eV, consists of four bands with a band gap of 2.36 eV, while the LUMO-HOMO gap of a picene molecule is 2.96 eV. These values are similar to those for solid coronene, with the difference being that the conduction band of solid picene originates from LUMO and LUMO+1 of an isolated picene molecule.<sup>8</sup> Considering the general tendency of LDA to underestimate band gaps, we expect that the actual band gap of coronene may be larger than the calculated value. An accurate prediction of optical properties and band widths will also require incorporation of many-body effects, as is done with the GW approximation by Roth *et al.*<sup>23</sup> for picene. The valence band of solid coronene has a width of 0.45 eV and consists of four bands; it is shown to be derived from the (again doubly-degenerate)  $e_{2u}$  HOMOs of an isolated coronene molecule.

**Downfolding.** We have constructed an *ab initio* tight-binding model from the maximally localized WFs<sup>11</sup> of the four-fold conduction band. The two-fold degenerate  $e_{1g}$  LUMOs for an isolated molecule have  $b_{3g}$  and  $b_{2g}$  symmetries in the  $D_{2h}$  representation. Figure 3(a) displays the two WFs localized at each of the molecules. While the downfolded tight-binding band (not shown) accurately reproduces the DFT-LDA band structure, we notice that the WF  $w_h$  is derived mainly from  $b_{3g}$  orbital while  $w_l$  comes from  $b_{2g}$ . The difference in the orbital energy between the two WFs is 18.2 meV, which is to be compared with 11.3 meV for solid picene. Figures 3(b) and 3(c) depict the major transfer integrals in the downfolded tight-binding model, which exhibit transfers along the  $b$  axis that are much stronger than along the other axes, in contrast to those in picene [see Fig. 3(c) in Ref. 8], for which two transfers on the  $a$ - $b$  plane are close to each other. The anisotropy of the transfers in coronene thus comes from the relative distances between the WFs.

**Doped solid coronene.** Let us finally discuss doped coronene. If we naively adopt a rigid-band picture for a doping level of  $x = 3$  for which superconductivity is observed, the Fermi surface (not shown) consists of multiple surfaces that comprise one-dimensional (planar) surfaces and a two-dimensional (cylindrical) one, along with a more three-dimensional one. However, since we have shown for doped picene<sup>8</sup> that the rigid-band picture is broken in this material for two reasons (i.e., a distorted herringbone structure upon doping along with a spilling of the molecular wave function over to potassium sites), we should have a look at the electronic structure of the coronene actually doped

with K. Since the structure of the doped system has not been experimentally obtained, we have tried a structural optimization of  $K_3$ coronene. Since this in itself is an important but vast task, here we only show a candidate structure. We started from a plausible geometry with one potassium atom just above the molecule and two in the interstitial region. The initial coordinates of the six potassium atoms we adopted are  $(1/2, 0, 0)$ ,  $(0, 1/2, 0)$ ,  $(\pm 1/3, 1/2, \pm 1/3)$ , and  $(\pm 5/6, 0, \pm 1/3)$ , which preserve the monoclinic symmetry. Interestingly, the optimization, with the lattice parameters fixed at those for the pristine structure, resulted in a significant rearrangement of the herringbone structure with the monoclinic symmetry lowered, along with a strong deformation of each molecule, as seen in Figs. 4(a) and 4(b). The band structure of  $K_3$ coronene is significantly more dispersive than the undoped one, where the LUMO-derived band group is fused with the upper band group, resulting in a much wider band group, as shown in Fig. 4(c). We can see that the resultant Fermi surface is an intriguing composite of one-dimensional surfaces (i.e., multiple pairs of planar surfaces) with different anisotropies. Doped picene also has multiple Fermi surfaces coexisting,<sup>8</sup> but doped coronene has a surface topology that is different from that in doped picene, which comes from different (and more one-dimensional) tight-binding structure [Figs. 3(b) and 3(c)]. The anisotropic, multiple Fermi surface should give a basis for examining superconductivity. In a phonon mechanism the problem becomes the coupling

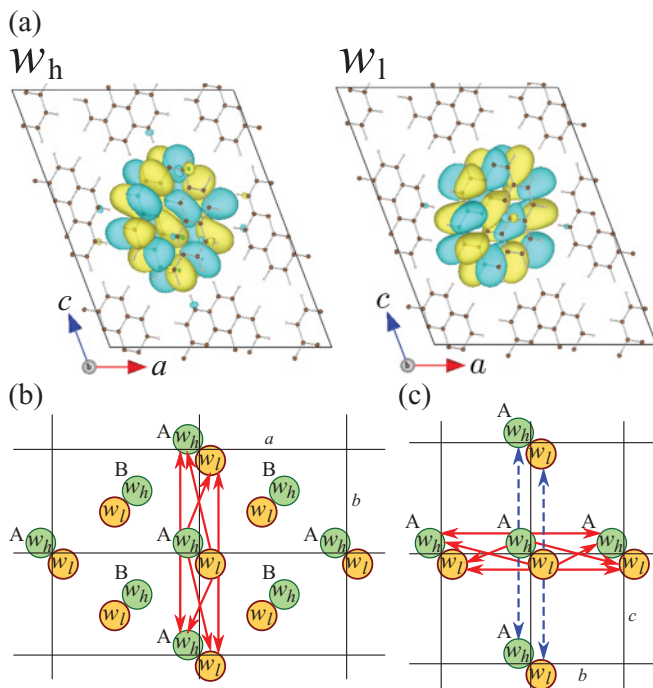


FIG. 3. (Color) (a) Maximally localized Wannier functions (right)  $w_l$  ( $w_h$ ) with lower-energy (higher-energy) constructed from the conduction bands of undoped solid coronene. Their transfer integrals  $t$  on the  $a$ - $b$  plane (b) and  $b$ - $c$  plane (c) are also shown, where the solid (dashed) arrows are for  $|t| > 30$  meV ( $10 < |t| < 30$  meV).

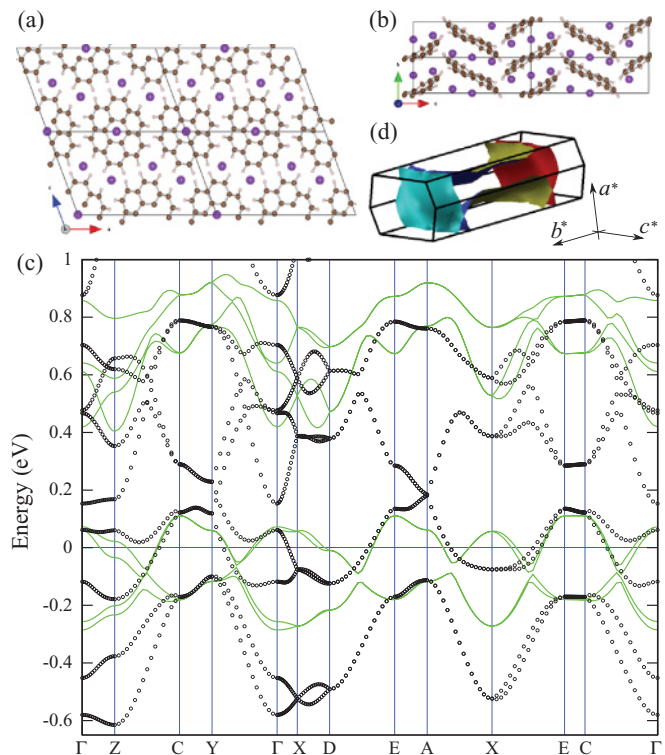


FIG. 4. (Color) Crystal structure of  $K_3$ coronene viewed along (a) the  $b$  and (b) the  $c$  axis. Larger balls represent K atoms. (c) Electronic band structures of  $K_3$ coronene (circles) and undoped coronene (curves). The origin of energy for the  $K_3$ coronene is set to its Fermi level while that for undoped coronene is set for  $x = 3$  in a rigid-band shift for comparison. (d) The Fermi surface for  $K_3$ coronene.

between the electrons on such a Fermi surface and the molecular phonons. The situation gives an interesting possibility for electron mechanisms as well, since the nesting between disconnected Fermi surfaces can give rise to a unique opportunity for an electron mechanism, especially in multiband cases.<sup>24</sup> For an accurate description of the structure more elaborate and exhaustive structural optimizations will be needed, since the large degrees of freedom on the dopant positions will render an energy surface with many local minima. Such a systematic examination is, however, beyond the scope of the present work and will be reported in future.

Finally, a few words about the “aromaticity” of molecules is in order. Its simplest definition is in terms of the “Clar sextets” (resonating benzene rings)<sup>25</sup> on a given molecular structure. When a molecule is fully benzenoid (where the sextets exhaust all the double bonds) the wave function tends to be localized on the sextets. In this picture picene is non-fully-benzenoid, while coronene, also non-fully-benzenoid, has multiple Clar structures.<sup>21</sup> The relation of these quantum chemical properties with band structures is another interesting future problem.

In summary, we have studied the electronic structure of solid coronene by means of first-principles calculations. The

conduction band is found to comprise four bands, which basically originate from the lowest two unoccupied molecular orbitals (doubly-degenerate, reflecting the molecular symmetry) in an isolated molecule, but the bands are entangled. The maximally localized WFs are used to derive a downfolded tight-binding Hamiltonian, where the major transfer integrals are found to significantly differ from those in solid picene. The Fermi surface for a candidate of the structure of  $K_x$  coronene with  $x = 3$ , for which superconductivity is found, comprises multiple sheets, as in doped picene but with different topology of the surface. Their relevance to superconductivity is an interesting future problem.

We are indebted to Yoshihiro Kubozono for letting us know of the experimental results prior to publication. The present work is partially supported by the Next Generation Supercomputer Project, Nanoscience Program from MEXT, Japan, and by Grants-in-aid for Scientific Research No. 19051016 and No. 22104010 from MEXT, Japan, and the JST PRESTO program. The calculations were performed at the supercomputer centers of ISSP, University of Tokyo, and at the Information Technology Center, University of Tokyo.

- 
- <sup>1</sup>R. Mitsuhashi, Y. Suzuki, Y. Yamanari, H. Mitamura, T. Kambe, N. Ikeda, H. Okamoto, A. Fujiwara, M. Yamaji, N. Kawasaki, Y. Maniwa, and Y. Kubozono, *Nature (London)* **464**, 76 (2010).
- <sup>2</sup>N. B. Hannay, T. H. Geballe, B. T. Matthias, K. Andres, P. Schmidt, and D. MacNair, *Phys. Rev. Lett.* **14**, 225 (1965).
- <sup>3</sup>T. E. Weller, M. Ellerby, S. S. Saxena, R. P. Smith, and N. T. Skipper, *Nature Phys.* **1**, 39 (2005); N. Emery, C. Hérold, M. d’Astuto, V. Garcia, Ch. Bellin, J. F. Marêché, P. Lagrange, and G. Loupiau, *Phys. Rev. Lett.* **95**, 087003 (2005).
- <sup>4</sup>A. F. Hebard, M. J. Rosseinsky, R. C. Haddon, D. W. Murphy, S. H. Glarum, T. T. M. Palstra, A. P. Ramirez, and A. R. Kortan, *Nature (London)* **350**, 600 (1991).
- <sup>5</sup>K. Tanigaki, T. W. Ebbesen, S. Saito, J. Mizuki, J. S. Tsai, Y. Kubo, and S. Kuroshima, *Nature (London)* **352**, 222 (1991).
- <sup>6</sup>T. T. M. Palstra, O. Zhou, Y. Iwasa, P. E. Sulewski, R. M. Fleming, and B. R. Zegarski, *Solid State Commun.* **93**, 327 (1995).
- <sup>7</sup>E. A. Ekimov, V. A. Sidorov, E. D. Bauer, N. N. Melfnik, N. J. Curro, J. D. Thompson, and S. M. Stishov, *Nature (London)* **428**, 542 (2004).
- <sup>8</sup>T. Kosugi, T. Miyake, S. Ishibashi, R. Arita, and H. Aoki, *J. Phys. Soc. Jpn.* **79**, 044705 (2010).
- <sup>9</sup>Y. Kubozono, M. Mitamura, X. Lee, X. He, Y. Yamanari, Y. Takahashi, Y. Suzuki, Y. Kaji, R. Eguchi, K. Akaike, T. Kambe, H. Okamoto, A. Fujiwara, T. Kato, T. Kosugi, and H. Aoki, submitted.
- <sup>10</sup>X. F. Wang, R. H. Liu, Z. Gui, Y. L. Xie, Y. J. Yan, J. J. Ying, X. G. Luo, and X. H. Chen, e-print [arXiv:1102.4075v1](https://arxiv.org/abs/1102.4075v1), have reported that  $K_x$  phenanthrene also exhibits superconductivity with  $T_c \simeq 5$  K.
- <sup>11</sup>N. Marzari and D. Vanderbilt, *Phys. Rev. B* **56**, 12847 (1997); I. Souza, N. Marzari, and D. Vanderbilt, *ibid.* **65**, 035109 (2001).
- <sup>12</sup>See, e.g., K. Kuroki, *J. Phys. Soc. Jpn.* **75**, 051013 (2006).
- <sup>13</sup>G. Giovannetti and M. Capone, *Phys. Rev. B* **83**, 134508 (2011).
- <sup>14</sup>M. Kim, B. I. Min, G. Lee, H. J. Kwon, Y. M. Rhee, and J. H. Shim, e-print [arXiv:1011.2712v1](https://arxiv.org/abs/1011.2712v1).
- <sup>15</sup>T. Kato and T. Yamabe, *J. Chem. Phys.* **115**, 8592 (2001); T. Kato, K. Yoshizawa, and K. Hirao, *ibid.* **116**, 3420 (2002); T. Kato and T. Yamabe, *Chem. Phys.* **325**, 437 (2006).
- <sup>16</sup>A. Subedi and L. Boeri, e-print [arXiv:1103.4020v1](https://arxiv.org/abs/1103.4020v1).
- <sup>17</sup>D. M. Ceperley and B. J. Alder, *Phys. Rev. Lett.* **45**, 566 (1980); J. P. Perdew and A. Zunger, *Phys. Rev. B* **23**, 5048 (1981).
- <sup>18</sup>P. E. Blöchl, *Phys. Rev. B* **50**, 17953 (1994); G. Kresse and D. Joubert, *ibid.* **59**, 1758 (1999).
- <sup>19</sup>[<http://www.qmas.jp/>].
- <sup>20</sup>T. Echigo, M. Kimata, and T. Maruoka, *Am. Mineral.* **92**, 1262 (2007).
- <sup>21</sup>T. M. Krygowski, M. Cyrański, A. Ciesielski, B. Świrski, and P. Leszczyński, *J. Chem. Inf. Comput. Sci.* **36**, 1135 (1996).
- <sup>22</sup>See Supplemental Material at <http://link.aps.org/supplemental/10.1103/PhysRevB.84.020507> for the optimized geometry.
- <sup>23</sup>F. Roth, M. Gatti, P. Cudazzo, M. Grobosch, B. Mahns, B. Büchner, A. Rubio, and M. Knupfer, *New J. Phys.* **12**, 103036 (2010).
- <sup>24</sup>H. Aoki, *Physica B* **404**, 700 (2009).
- <sup>25</sup>E. Clar, *Polycyclic Hydrocarbons* (Academic, London, 1964).